ELSEVIER

Thermochimica Acta 387 (2002) 153–171

thermochimica acta

www.elsevier.com/locate/tca

Reactivity in the system copper–arsenic–sulfur I. The formation of Cu_3AsS_4, enargite

A. Müller, R. Blachnik*

Institut für Chemie, Universität Osnabrück, Barbarastraße 7, D49069 Osnabrück, Germany

Received 29 August 2001; accepted 12 November 2001

Abstract

The reaction pathways in the synthesis of Cu_3AsS_4 have been studied in the DTA in the range 25–870 °C with a heating rate of 10 K/min. Educts, intermediates and products were characterised by X-ray diffraction. Educts were the elements and the binary compounds $Cu_{3-x}As$, $Cu_{5-\delta}As_2$, As_4S_4, As_2S_3, the two copper(I) sulfides $Cu_{1.91}S$, Cu_2S, and CuS. The 19 examined educt mixtures are divided by their thermal effects during reaction into three groups. Mixtures of the group I have low copper or copper arsenide contents. Educts in group II are mainly copper arsenides and sulfur, and educts of group III enclose all other mixtures, including that from the elements. In all cases the reaction to Cu_3AsS_4 proceeds stepwise. The various intermediates are mainly the binary compounds CuS and As_4S_4 at lower temperatures and at higher temperatures the ternary compounds $Cu_6As_4S_9$, $Cu_4As_2S_5$ or $Cu_{12+x}As_{4+y}S_{13}$. The synthesis is complete at approximately 600 °C. Heating above the melting point of Cu_3AsS_4 at 694 °C increases the amount of by-products.

In grinding and ageing experiments copper arsenides react with sulfur, As_2S_3, and CuS to metastable Cu_2As. The reaction between $Cu_{3-x}As + S$ does not proceed by treatment in a planetary ball mill. $As_4S_4 + CuS$ do not react during mediumised milling, but the formation of Cu_3AsS_4 occurs after this treatment in one step in the DTA run. The desoxidation of copper powders is a decisive influence factor for the reaction from the elements.

Keywords: Solid state reaction; Reactivity; Sulfo salts; Enargite; Copper arsenic sulfide

1. Introduction

Crystalline and amorphous chalcogenides were subjected to numerous investigations because their physical properties are of technical importance. In addition systems with sulfur are of interest in mineralogy and geology and give information about the physical conditions on earth at their genesis. For these reasons, phase equilibria of binary and ternary sulfur systems were often investigated. Less information is known on reaction pathways and conditions on which elements or compounds react to binary and ternary sulfides. To our knowledge in the past only three publications [1–3] dealt with reaction pathways in the system Cu–As–S, though it contains compounds which are important copper and arsenic ores [4,5].

In view of this gap we investigated the pathways on which the compound Cu_3AsS_4 is formed. Besides the elements, the binary compounds $Cu_{3-x}As$, $Cu_{5-\delta}As_2$, As_4S_4, As_2S_3, two copper(I) sulfides ('$Cu_{1.91}S$', Cu_2S), and CuS were used as educts. The reactions were detected in situ by thermoanalytical and X-ray methods. Examined parameters were mechanical treatment, purification of copper, and ageing.

* Corresponding author. Fax: +54-19693323.
E-mail address: bl@chnik.de (R. Blachnik).

0040-6031/02/$ – see front matter
PII: S0040-6031(01)00837-1

2. The ternary system Cu–As–S

Although several authors [6–13] have examined parts of the system, Rikel' et al. [14] could give the phase relations only schematically because of contradictory results.

The system is characterised by three miscibility gaps and five ternary compounds, Cu_3AsS_4, $Cu_{12+x}As_{4+y}S_{13}$, $Cu_4As_2S_5$, $Cu_6As_4S_9$, and CuAsS, of which the last three decompose pericteCtially. The primary crystallisation fields of $Cu_{2-x}S$, As, Cu_3AsS_4, and $Cu_{12+x}As_{4+y}S_{13}$ dominate the Gibbs triangle (Fig. 1). The sections As–Cu_2S [9,11,12], As–Cu_3AsS_3 [13], Cu_2S–Cu_3As [8,13], and Cu_2S–As_2S_3 [8,13] are reported as quasibinaries. However, Rikel' et al. [14] accepted this character only of the sections As–Cu_2S and Cu_2S–As_2S_3.

With the exception of $Cu_4As_2S_5$ all compounds exist as minerals, which are characterised by covalent As–S bonds and which crystallise in superstructures of the sphalerite or wurtzite type [12,15,16]. The structure of enargite is characterised by AsS_4 tetrahedra, whereas the compounds on the section Cu_2S–As_2S_3 contain trigonal AsS_3 pyramids.

Orthorhombic Cu_3AsS_4, enargite, has at higher temperature a small homogeneity range [9]. The melting behaviour is not clear. Kurz [12] assumed a peritectic decomposition into $Cu_{12+x}As_{4+y}S_{13}$ and melt at 642 °C, Maske and Skinner [9] found congruent melting at 672 °C. All available thermal data are summarised in Table 1. A second form, tetragonal luzonite is a metastable high-pressure modification [17].

$Cu_{12+x}As_{4+y}S_{13}$, tennantite, and its multinary varieties are widely spread in nature. Since the compound

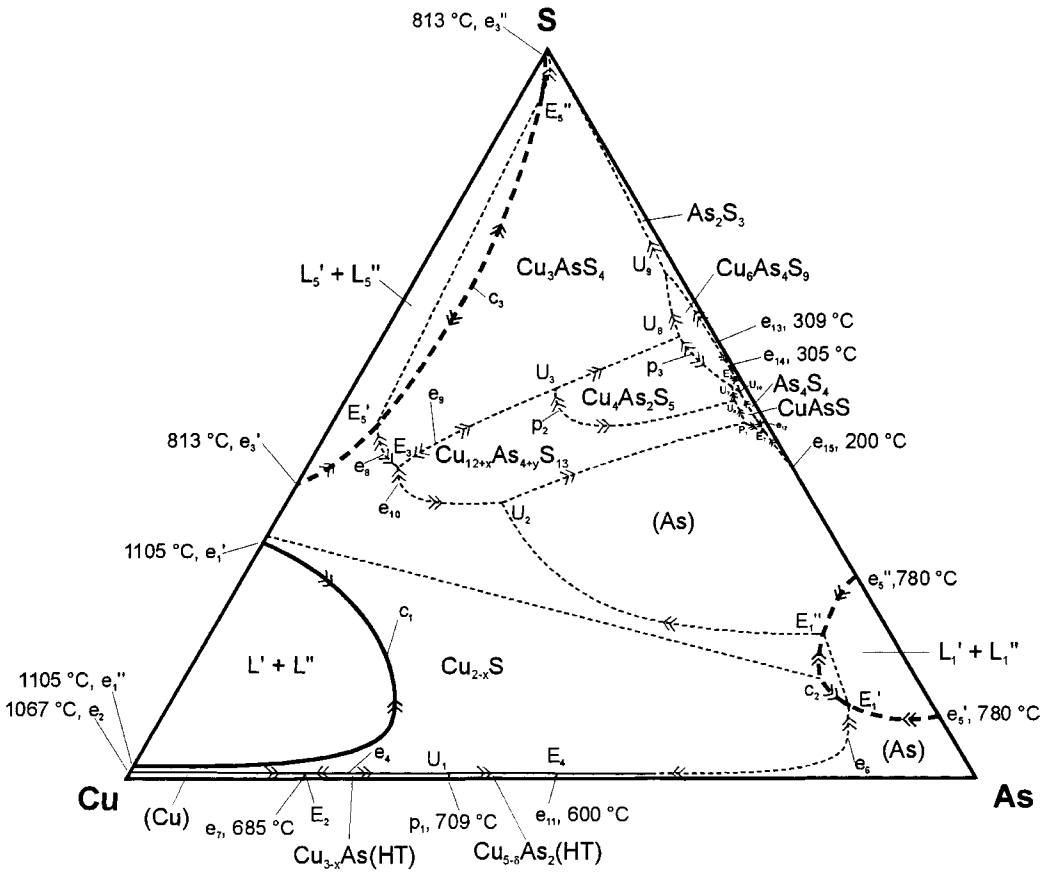

Fig. 1. Liquidus projection of the system Cu–As–S [14].

Table 1
Melting behaviour of Cu_3AsS_4 and $Cu_{12+x}As_{4+y}S_{13}$ from the literature

Cu_3AsS_4	$Cu_{12+x}As_{4+y}S_{13}$[a]
$Cu_3AsS_4 \rightleftarrows L$	$Cu_{12+x}As_{4+y}S_{13} \rightleftarrows L$
655 °C [34]	640 °C [34]
$Cu_3AsS_4 \rightleftarrows L$	$Cu_{12+x}As_{4+y}S_{13} \rightleftarrows L$
689 °C[b] [8]	665 °C[c] [9]
$Cu_3AsS_4 \rightleftarrows Cu_{12+x}As_{4+y}S_{13} + S$	$Cu_{12+x}As_{4+y}S_{13} \rightleftarrows CuAsS + S$
672 °C[d] [8]	710 °C [35]
$Cu_3AsS_4 \rightleftarrows L$	$Cu_{12+x}As_{4+y}S_{13} \rightleftarrows Cu_2S + As_2S_3$
672 °C [9]	670 °C [1]
$Cu_3AsS_4 \rightleftarrows Cu_{12+x}As_{4+y}S_{13} + L$	$Cu_{12+x}As_{4+y}S_{13} \rightleftarrows L$
642 °C [12]	656 °C [13]
$Cu_3AsS_4 \rightleftarrows Cu_{12+x}As_{4+y}S_{13} + S_2(g)$	$Cu_{12+x}As_{4+y}S_{13} \rightleftarrows L$
590 °C [36]	637 °C [36]
$Cu_3AsS_4 \rightleftarrows Cu_{12+x}As_{4+y}S_{13}$	$Cu_{12+x}As_{4+y}S_{13} \rightleftarrows L$
655 °C [3]	670 °C [3]

[a] If not otherwise stated composition was Cu_3AsS_3.
[b] Sealed ampoule.
[c] Composition of congruent melting compound: $Cu_{12.31}As_4S_{13}$.
[d] Open crudble.

contains Cu(I) and Cu(II) it is better represented by the formulae $Cu(I)_{10}Cu(II)_2As_4S_{13}$ [18] with a homogeneity range ($0 \leq x \leq 1.72, 0 \leq y \leq 0.08$) according to Maske and Skinner [9]. Kurz and Blachnik [13] observed in the same region Cu_3AsS_3, which exists in a high- and low-temperature form. Small homogeneity ranges were found for both modifications with a maximum range in molar fraction of $x_{Cu_2S} = 0.04$ in the low- and $x_{Cu_2S} = 0.02$ in the high-temperature form. The low-temperature modification was identified as a superstructure of tennantite. The melting behaviour of tennantite is also reported in Table 1. Rikel' et al. [14] enlarged in their assessment the phase field of $Cu_{12+x}As_{4+y}S_{13}$ so that it includes the composition Cu_3AsS_3.

$Cu_4As_2S_5$ has a narrow homogeneity range [13] including $Cu_{24}As_{12}S_{31}$, which was found by Maske and Skinner [9]. $Cu_4As_2S_5$ decomposes peritectically at 597 °C into $Cu_{12+x}As_{4+y}S_{13}$ and melt [13,14]. Preliminary studies of the crystal structure revealed a sphalerite-substructure with monoclinic symmetry [12].

Synthetic $Cu_6As_4S_9$ corresponds to the mineral sinnerite [17]. The compound decomposes at 530 °C into $Cu_4As_2S_5$ and melt [13]. CuAsS (lautite) will be described in a following paper.

3. Experimental

3.1. Methods

The thermal analyses were performed with a DTA device, developed by Gather [19]. The thermocouples (Ni/CrNi) were calibrated with the melting points of gallium, indium, lead, antimony, and silver. The samples were sealed in evacuated silica ampoules (length 3.5 cm; diameter 4.0 mm; wall thickness 0.5 mm). The runs were done with a heating rate of 10 K/min, a sample mass of 0.12–0.18 g, and silicon as reference. A DSC 404C Pegasus (Netzsch, high-temperature furnace; DSC sensor with Pt10%/Pt-Rh thermocouples) was used for small heating rates and calibrated with indium, tin, lead, antimony, and silver. The samples with a mass of about 100 mg were measured in evacuated and sealed silica crucibles (length 15 mm; diameter 6.3 mm; wall thickness 0.4 mm). An empty silica crucible served as reference. The temperatures of effects were determined from the onset of the peaks. X-ray measurements were carried out with the aid of a transmission powder diffractometer STADI P (Stoe), using Cu $K_{\alpha 1}$ radiation (154.051 pm), a germanium single crystal monochromator, and a linear position sensitive detector. Temperature dependent X-ray measurements were performed with a high-temperature attachment. The temperature was increased in 10 °C steps. After heating in 10 min to the next temperature followed an equilibration period of 36 min. At room temperature a Huber Vertical Guinier Camera 620 and at high temperatures an Enraf Nonius Guinier Simon Camera FR 553 (heating rate 0.17 K/min) were used. For the high-temperature measurements the samples were placed in evacuated and sealed silica capillaries. X-ray measurements were interpreted by comparison with the PDF-2 database of JCPDS-International Centre for Diffraction Data [20] or by simulation of XRD patterns with single crystal data from ICSD [21]. Both procedures were performed with the program VISUAL X^{POW} [22].

Microscopic investigations were done with a microscope (Olympus) with a maximum magnification of 40×.

3.2. Chemicals

Elements used are described in Table 2. A more detailed analyses is given in [23]. Arsenic was

Table 2
Elements used in this work

Element	Source	Shape	Purity (%)[a]	Purification method
Arsenic	Preussag	Pieces	99.9995	Oxides sublimed
Copper[b,c]	Heraeus	Powder	99.8	Reduced at 260 and 650 °C
Copper[d]	ABCR	Shot	99.999	Reduced in ethanol
Copper[e]	Goodfellow	Foil	OFHC[f], 99.95	Reduced in ethanol
Sulfur	Merck	Powder	–	Recrystallised

[a] Only metallic impurities.
[b] Used for reaction mixtures.
[c] Main particle size, $d = 36$–$100\ \mu m$. Determined by a analytical sieve shaker.
[d] Used for '$Cu_{1.91}S$', CuS, $Cu_{5-\delta}As^{*}$', $Cu_{3-x}As$.
[e] Used for CuS, Cu_2S, $Cu_{3-x}As$.
[f] Oxygen-free high conductivity.

desoxidised by subliming arsenic oxide in an evacuated silica tube in a temperature gradient (300 °C → room temperature) for several days. A mixture of 90% N_2 and 10% H_2 was passed over copper powders for desoxidation for 0.5 h at 260 °C or for 4 h at 650 °C in a silica tube. If not otherwise mentioned copper powder reduced at 260 °C was used. Oxide layers on copper foils or shot were removed by dipping the hot metal which was pre-heated in argon atmosphere into ethanol. Sulfur was recrystallised twice from CS_2. The product was then treated in vacuum at 150 °C for 0.5 h to remove solvent and traces of water. After purification the elements were stored under argon.

All educts were prepared from the elements in evacuated silica ampoules or tubes. Copper arsenides and arsenic sulfides were synthesised by heating stoichiometric amounts of the elements to the melting or boiling points of each element. These temperatures were kept for 1 day. The samples were then heated for a few hours above the melting-point of the corresponding compound, quenched in ice-water, and if necessary annealed and quenched again. As_4S_4 was then sublimed for purification.

Two copper(I)-sulfides were synthesised: '$Cu_{1.91}S$', positioned in the centre of the homogeneity region of $Cu_{2-x}S$ and congruently melting $Cu_{2-x}S$. They were prepared by heating copper shot or foils at 800 °C and sulfur at 440 °C for 2 weeks on opposite ends of a silica tube [24] and homogenising the product for 2 days at 800 °C for '$Cu_{1.91}S$' and for Cu_2S for 2 days at 350 °C and for 5 days at 90 °C.

CuS was synthesised similarly within 8 days using 450 °C for the copper reservoir and 425 °C for the sulfur reservoir (method I) or by heating the elements in a flame, followed by homogenisation at 450 °C (method II).

Ternary compounds were synthesised by annealing the constituent elements for 2 weeks at 480 °C and for 1 week at 300 °C followed by quenching and grinding. After that pellets were fabricated and annealed for 5 months at 320 °C.

3.3. Preparation and measurement

Samples with the composition Cu_3AsS_4 were obtained by mortaring corresponding amounts of the elements or of binary compounds.

Quartz ampoules were heated in vacuum to remove water, flushed with argon, and then filled with these mixtures. During sealing, the end of the ampoule was cooled to prevent reaction. Immediately after sealing the samples were used for thermal analyses to avoid ageing effects.

Thermal effects were characterised with ex-situ X-ray measurements by quenching samples from the temperatures of the onset, the maximum and the end of the effect in ice-water mixture. These samples were mixed with SiO_2 as standard in a mass ratio of 1:9 and examined by X-ray experiments to determine the change of concentrations of reaction products.

Mechanical alloying was performed with a planetary ball mill (Pulverisette 7, Fritsch) with hard-metal tungsten carbide bowls ($V = 12$ ml) and milling balls ($\varnothing$ 12 mm) in argon. The rotational speed was 400 min^{-1}. The mass of samples was approximately 4 g. The mill was stopped after 1, 2, 5, 10, 20, 30, 40,

50, and 60 min and parts of the mixture were taken for X-ray and DTA examination. The samples were handled in nitrogen atmosphere in a glove box to avoid oxidation of sensitive intermediate products.

In ageing experiments ground reaction mixtures were stored 3 years under argon atmosphere in the dark.

4. Results and discussion

4.1. General aspects

4.1.1. Characterisation of educts

The knowledge of the thermal properties of the educts is helpful to interpret the course of the reaction. In Table 3, literature data are compared with our results. Details of the different copper and sulfur charges were previously published [23].

Congruently, melting $Cu_{3-x}As$ was obtained in form of the trigonal low-temperature modification. The identity with previously reported $Cu_{3-x}As$(LT) [25] was confirmed by a comparison of the X-ray reflections with those calculated from single crystal data [26].

Subramanian and Laughlin [27] reported the formula $Cu_{4.90}As_2$ for incongruently melting $Cu_{5-\delta}As_2$(LT), however, we obtained with educts of this composition always two-phase mixtures. A nearly pure compound was prepared using the composition $Cu_{4.75}As_2$ reported by Juza and Benda [28]. Traces of $Cu_{3-x}As$(LT) reveal that the eutectoid decomposition cannot completely be suppressed by quenching.

The preparation of As_2S_3 yielded metastable glasses, which needed long recrystallisation times. Structure determining elements are corner-sharing AsS_3-pyramids [29,30].

Sublimation of As_4S_4 raw products yielded a mixture of α- and β-As_4S_4, both modifications contain As_4S_4 molecules. The melting point of β-As_4S_4 was lowered by a slight contamination with alacranite, As_8S_9. A shoulder of the melting peak in the DTA runs is probably caused by the As_4S_4–As_2S_3 eutectic at 305 °C [31].

Both, $Cu_{2-x}S$ and '$Cu_{1.91}S$', decomposed at room temperature into a two-phase mixture of stable and metastable copper(I)-sulfides as expected from the literature cited in [23]. The melting point of Cu_2S was found 12 °C below the literature value.

4.1.2. Thermal behaviour of Cu_3AsS_4

Cu_3AsS_4 melts congruently at 694 °C with a heating rate of 10 K/min of the DTA. With a lower heating rate (0.2 K/min) the peak at 687 °C has the shape of a liquidus effect. These temperatures agree with the value of 689 °C of Cambi and Elli [8]. The cooling

Table 3
Characterisation of educts

Educt	x_{Cu} or x_{As}	Thermal data from literature (°C)	Thermal data in this work (°C)	Identified substance by XRD[a]	Appearance
As	1.000	No[b]	No	As [37]	Gray luster
$Cu_{3-x}As$	0.738	827 [38]	833	$Cu_{3-x}As$(LT) [25,26]	Silvery metallic luster
$Cu_{5-\delta}As_2$	–[c]	300, 380, 709, ≈810 [38]	302, 390, 717, 804, 818	$Cu_{5-\delta}As_2$(LT)[d] [39,40], $Cu_{3-x}As$(LT)(↓)	Metallic luster
As_4S_4	–[e]	266, 318 [31]	268, 305, 311	α-As_4S_4 [41,42], β-As_4S_4[d] [43,44], As_8S_9[d](↓) [45]	Orange
As_2S_3	0.400	No	No	Amorphous[d]	Dark-red, transparent
CuS	0.500	507 [46]	512	CuS [47]	Dark-blue
Cu_2S	0.666	≈90, ≈98, ≈415, 1130 [46]	91, 101, 410, 1118	α-Cu_2S [48], $Cu_{1.96}S$[d](↓) [49]	Gray
'$Cu_{1.91}S$'	0.657	93, ≈1110 [46]	91, 1106	$Cu_{1.81}S$[d] [50], $Cu_{1.95}S$ [51]	Gray

(↓) Very low concentration.
[a] Phases in order of intensities of reflections.
[b] Not heated up to triple point.
[c] Arsenic rich border of homogeneity range.
[d] At room temperature metastable phases.
[e] No value given, because sublimed.

curve has in all cases three thermal effects. This behaviour can be explained by an evaporation of sulfur on heating. During freezing gaseous sulfur cannot equilibrate with the bulk material so that in these samples a mixture of Cu_3AsS_4, $Cu_4As_2S_5$, and $Cu_{12+x}As_{4+y}S_{13}$ is formed.

$Cu_{12+x}As_{4+y}S_{13}$ (actual composition Cu_3AsS_3) has a melting point of 658 °C, in accordance with data of Kurz and Blachnik (656 °C) [13]. Thus the melting point of $Cu_{12+x}As_{4+y}S_{13}$ is lower than that of Cu_3AsS_4 and a peritectic decomposition of Cu_3AsS_4 can be excluded.

4.1.3. Mechanical treatment and ageing

Mixtures of two components were homogenised by mortaring and examined by X-ray diffractometry to investigate if reactions take place during mortaring. Table 4 reveals that copper arsenides react with sulfur, As_2S_3, and CuS, respectively, to metastable Cu_2As. The reaction with sulfur is complete within minutes.

These reactions, initiated by mortaring, advance during ageing. Generally Cu_2As is the main ageing product, CuS was found as a second product after ageing of copper arsenides with sulfur, whereas the reaction between copper arsenides and CuS leads to Djurleit or α-Cu_2S. Reaction equations with $Cu_{3-x}As$(LT) as educt are:

$$Cu_{3-x}As(LT) + \frac{(1-x)}{8}\alpha\text{-}S_8 \rightarrow Cu_2As + (1-x)CuS$$

$$Cu_{3-x}As(LT) + (1-x)CuS \rightarrow Cu_2As + (1-x)Cu_2S$$

An estimation of the enthalpies of reaction with available data ($\Delta H_f(Cu_{3-x}As) = -14$ kJ mol^{-1} [32]; $\Delta H_f(CuS) = -53$ kJ mol^{-1} [33]; $\Delta H_f(Cu_2S) = -81$ kJ mol^{-1} [33]) revealed that both reactions are probably exothermic despite the formation of metastable Cu_2As.

4.1.4. Classification of reaction mixtures

Table 5 lists the thermal data gained from DTA runs up to 870 °C and the final products as identified in X-ray diffractograms. The results of temperature dependent X-ray measurements are summarised in Table 6.

The educt mixtures can be divided in three groups. The educts of group I have low copper or copper arsenide content. Educts in group II contain mainly copper arsenides and sulfur. In group III all other educt mixtures are found.

Mixtures of the group I are characterised by a start of the reaction at 330 ± 6 °C (with the exception of CuS + As + S) and four or less exothermic reaction effects. In addition two endothermic effects are observed which correspond to the melting of As_4S_4 at 300 ± 1 °C and the peritectic decomposition of CuS at 504 ± 6 °C. Not all mixtures contained initially As_4S_4 or CuS, therefore they form also as intermediates on heating. The observed melting point of As_4S_4 is about 20 °C lower than that of pure As_4S_4, probably caused by contamination with arsenic sulfides of higher sulfur contents. A decrease of reaction temperatures was observed in temperature dependent Guinier powder diffractograms, due to the much lower

Table 4
Phases identified by XRD in ground or aged reaction mixtures with two components

Reaction mixture	Grinding[a]	Ageing[a]
$Cu_{3-x}As + As_2S_3$	$Cu_{3-x}As$(LT), $Cu_{5-\delta}As_2$(LT)(↓)	Not examined
$Cu_{3-x}As + S$	α-S_8 [52], Cu_2As [53], CuS(↓)	Cu_2As, α-S_8, CuS
$Cu_{3-x}As + CuS$	CuS, $Cu_{3-x}As$(LT), Cu_2As	Cu_2As, As_2O_3 [54], Cu_2S
$Cu_{5-\delta}As_2 + As_4S_4$	No reaction	$Cu_{5-\delta}As_2$(LT), α-As_4S_4, Cu_2As
$Cu_{5-\delta}As_2 + As_2S_3$	Cu_2As, $Cu_{5-\delta}As_2$(LT)[b]	Cu_2As, As_2O_3[c]
$Cu_{5-\delta}As_2 + S$	α-S_8, Cu_2As	Cu_2As, α-S_8, CuS
$Cu_{5-\delta}As_2 + CuS$	CuS, $Cu_{5-\delta}As_2$(LT), Cu_2As	Cu_2As, CuS, $Cu_{1.95}S$
$As_2S_3 + Cu_2S$	No reaction	$Cu_{1.95}S$, α-Cu_2S

(↓) Very low concentration.
[a] Phases in order of intensities of reflections.
[b] After grinding and pressing into pellets.
[c] Because of the long storage period, the formation of As_2O_3 was sometimes unavoidable.

Table 5
Results of thermal experiments and corresponding products

Reaction mixture	Mass fraction (%)			Temperature of exothermic effect (°C)	Identified phases by XRD[a]
Group I					
$CuS + As_4S_4$	73	27		331, 380(↓), 459(↑), 514	Cu_3AsS_4 [15,55], $Cu_{12+x}As_{4+y}S_{13}$ [56][b], $Cu_4As_2S_5$(↓) [12]
CuS[c] + As + S	73	19	8	255(↑), 426	Cu_3AsS_4
CuS[c] + As_2S_3 + As	73	21	6	331, 475, 501(↑)	Cu_3AsS_4, $Cu_{12+x}As_{4+y}S_{13}$, $Cu_4As_2S_5$(↓)
CuS[c] + As_2S_3 + $Cu_{3-x}As$	65	28	7	322, 436(↓), 513(↑)	Cu_3AsS_4, $Cu_{12+x}As_{4+y}S_{13}$, $Cu_4As_2S_5$(↓)
CuS + As_2S_3 + $Cu_{5-\delta}As_2$	65	27	7	329, 377, 473, 485(↑)	Cu_3AsS_4, $Cu_{12+x}As_{4+y}S_{13}$, $Cu_4As_2S_5$(↓)
CuS + As_2S_3 + '$Cu_{1.91}S$'	47	31	21	324, 367, 438(↓), 513(↑)	Cu_3AsS_4, $Cu_{12+x}As_{4+y}S_{13}$, $Cu_4As_2S_5$
'$Cu_{1.91}S$' + As_2S_3 + S	61	31	8	342, 520(↑), 539(↓)	Cu_3AsS_4, $Cu_{12+x}As_{4+y}S_{13}$
Group II					
$Cu_{3-x}As$ + S + Cu[d]	64	33	3	70, 161(↑), 275, 306, 434, 480(↓)	$Cu_{12+x}As_{4+y}S_{13}$, Cu_3AsS_4, $Cu_4As_2S_5$
$Cu_{3-x}As$ + S + CuS[c]	64	31	5	162(↑), 279, 312, 514	Cu_3AsS_4, $Cu_{12+x}As_{4+y}S_{13}$, $Cu_4As_2S_5$(↓)
$Cu_{3-x}As$ + S + '$Cu_{1.91}S$'	64	32	4	159(↑), 291, 340, 515	$Cu_{12+x}As_{4+y}S_{13}$, Cu_3AsS_4, $Cu_4As_2S_5$(↓)
$Cu_{5-\delta}As_2$ + S + Cu	58	33	9	157(↑), 252, 309, 566	$Cu_{12+x}As_{4+y}S_{13}$, Cu_3AsS_4, $Cu_4As_2S_5$
$Cu_{5-\delta}As_2$ + S + CuS	59	28	13	154(↑), 279, 300, 358, 526	Cu_3AsS_4, $Cu_{12+x}As_{4+y}S_{13}$, Cu_4As_2S5(↓)
$Cu_{5-\delta}As_2$ + S + '$Cu_{1.91}S$'	58	30	11	157(↑), 267, 378, 515, 547	$Cu_{12+x}As_{4+y}S_{13}$, Cu_3AsS_4, Cu_4As_2S5(↓)
Group III					
Cu +S + As	48	33	19	164, 191(↑), 255, 333, 373	Cu_3AsS_4, $Cu_{12+x}As_{4+y}S_{13}$, $Cu_4As_2S_5$
Cu[d] +S + As	48	33	19	81, 165, 195(↑), 260, 524	Cu_3AsS_4, $Cu_4As_2S_5$, $Cu_{12+x}As_{4+y}S_{13}$
Cu +As_2S_3 + S	48	31	20	88(↓), 220(↑), 303	$Cu_{12+x}As_{4+y}S_{13}$, Cu_3AsS_4, $Cu_4As_2S_5$(↓)
Cu +As_4S_4 + S	48	27	24	197, 227, 325(↑)	Cu_3AsS_4, $Cu_{12+x}As_{4+y}S_{13}$, $Cu_4As_2S_5$(↓)
CuS +As_2S_3 + Cu	61	31	8	94(↓), 142(↑), 236(↓), 286, 323, 350, 503	Cu_3AsS_4, $Cu_{12+x}As_{4+y}S_{13}$, $Cu_4As_2S_5$
Cu_2S +S + As	61	20	19	149, 196, 224, 261, 343(↑), 430, 512	$Cu_{12+x}As_{4+y}S_{13}$, Cu_3AsS_4, $Cu_4As_2S_5$
'$Cu_{1.91}S$' +As_4S_4 + S	61	27	12	134, 247, 337, 514(↑), 573(↓)	Cu_3AsS_4, $Cu_{12+x}As_{4+y}S_{13}$, $Cu_4As_2S_5$(↓)

(↓) Small peak or very low concentration; (↑) the largest peak in the DTA curve.
[a] Phases in order of intensities of reflections.
[b] Simulated XRD-pattern with single crystal data of the mineral binnite, $Cu_{12}As_4S_{13}$.
[c] CuS prepared according to method I.
[d] Copper powder reduced at 650 °C.

heating rates. The observed primary ternary compound was always $Cu_6As_4S_9$.

Mixtures of the group II are characterised by a strong exothermic effect at 158 ± 3 °C at lower temperature than that in group I. It is followed by at least two smaller overlapping effects. In most runs incongruent melting of CuS was detected. Copper arsenides determine the course of reaction, because the influence of the third component is small due to its low content.

The products of all groups after the DTA measurements were parts of the three-phase field Cu_3AsS_4–$Cu_{12+x}As_{4+y}S_{13}$–$Cu_4As_2S_5$, in accordance with the melting behaviour of Cu_3AsS_4 (see Section 4.1.2). $Cu_{12+x}As_{4+y}S_{13}$ was the main product in some sulfur rich educts. In special runs the educt mixtures were heated to 600 °C and than molten in a consecutive run. An exothermic reaction effect was never observed in the second run. But the amount of by-products increased which were present in traces or even absent in the first run. Thus melting of the sample is disadvantageous for the preparation of Cu_3AsS_4.

4.2. CuS and As_4S_4 as educts

4.2.1. Thermal synthesis

The reaction pathway of group I is described with the aid of the educt mixture CuS + As_4S_4. Fig. 2 presents the DTA trace and the marking of thermal effects. Table 7 contains the products found in quenched samples by subsequent X-ray or microscopic examination.

Table 6
Results of temperature dependent Guinier photographs

Reaction mixture	Examined temperature region (°C)	Temperature region of educts and products (°C)							
		As	CuS	Other educts	$Cu_{2-x}S$ [57,58]	$Cu_6As_4S_9$	$Cu_{12+x}As_{4+y}S_{13}$	Cu_3AsS_4	Other products
Group I									
$CuS + As_4S_4$	150–710		To 340	As_4S_4: to 300		300–440		From 370 to 390(↑), 560(↑)	
$CuS + As + S$	130–710	To 240	300(↓) to 490			220–420	From 680	From 430 to 460(↑), 510(↑)	
$CuS + As_2S_3 + Cu_{3-x}As$	150–710		To 310			250–380		From 330 to 370(↑)	
$CuS + As_2S_3 +$ '$Cu_{1.91}S$'	80–740		290(↓) to 410		To 200[a]	220–410		360–680	
Group II									
$Cu_{3-x}As + S + Cu$	80–750	160–260	110–310	α-S_8: to 80	270–410	310–410	390–700		Cu_2As[b]: to 110 $Cu_4As_2S_5$: 410–550
$Cu_{3-x}As + S$	50–680	150–250	90–370 300(↓)	α-S_8: to 80	280–450	310–390	From 420	From 400	Cu_2As: to 130 $Cu_4As_2S_6$: 400–510
$Cu_{3-x}S + S + CuS$	120–370		To 280		240–300	From 280			Cu_2As: to 130
Group III									
$Cu + S + As$	70–370	To 270	90–200	Cu: 180(↓) to 210	From 180		From 250 to 310(↓)		
'$Cu_{1.91}S$' + As_4S_4 + S	80–750		310(↓) to 420	α-S_8: to 80 α-As_4S_4: to 240	200–320	200–430		400–720	$Cu_4As_2S_5$: from 250 to 310(↓)

(↓) Decrease of intensity of reflections; (↑) increase of intensity of reflections.
[a] Above 90 °C, '$Cu_{1.91}S$' exists mainly as $Cu_{2-x}S$.
[b] $Cu_{3-x}S$ reacts during grinding with sulfur to Cu_2As.

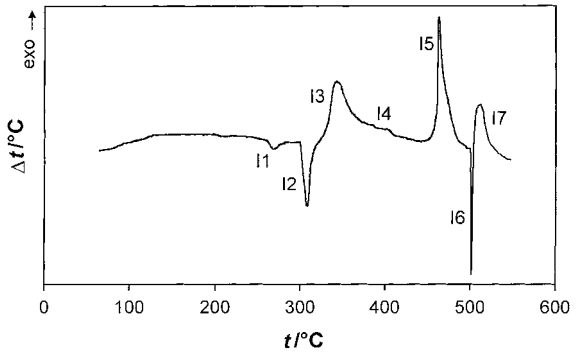

Fig. 2. DTA trace of the reaction mixture CuS + As_4S_4.

The sequence of reactions can be followed with the aid of the reaction equations in Fig. 3. The stoichiometric coefficients were estimated for each compound from the intensities of reflections in the diffractograms and those of the thermal effects in the DTA runs.

The first thermal effect (I1) is due to the α–β transition of As_4S_4 at 262 ± 2 °C followed by melting of β-As_4S_4 at 301 ± 2 °C (I2), traces of $Cu_6As_4S_9$ are already formed. The main reaction to this compound in which As_4S_4 is consumed and sulfur liberated starts at 331 ± 2 °C (I3). A shoulder at 380 ± 4 °C (I4) is observed in the declining flank of I3 in most runs. The sample consists after this effect of coagulated black particles. CuS reacts at 459 ± 5 °C with intermediate $Cu_6As_4S_9$ to Cu_3AsS_4 (I5). This reaction is not complete because product layers separate the educts. The amount of Cu_3AsS_4, which is formed, depends on synthesis conditions of the educt CuS. After the peritectic decomposition of CuS into $Cu_{2-x}S$ and sulfur at 511 ± 5 °C (I6) the reaction to Cu_3AsS_4 is completed within the exothermic effect at 514 ± 8 °C (I7). $Cu_{2-x}S$ is not observed in X-ray experiments which indicates that it is consumed instantly.

Table 7
Phases observed in quenched samples of the reaction mixture CuS + As_4S_4

Interruption of the reaction	Phases
After grinding, before heating	CuS, β-As_4S_4, α-As_4S_4
Before I1	CuS, β-As_4S_4, α-As_4S_4(↓)
Before I2	CuS, β-As_4S_4
After I2	CuS, β-As_4S_4, $Cu_6As_4S_9$(↓)
Before I3	CuS, β-As_4S_4, $Cu_6As_4S_9$(↓)
During I3	CuS, β-As_4S_4, $Cu_6As_4S_9$, S[a](↓)
After I3	CuS, $Cu_6As_4S_9$, β-As_4S_4(↓), S(↓)
During I4	$Cu_6As_4S_9$, CuS, β-As_4S_4(↓), S(↓)
After I4	CuS, $Cu_6As_4S_9$, Cu_3AsS_4(↓), S(↓)
Before I5	$Cu_6As_4S_9$, CuS, Cu_3AsS_4, S(↓)
During I5	Cu_3AsS_4, CuS, $Cu_6As_4S_9$, S(↓)
After I5	Cu_3AsS_4, $Cu_6As_4S_9$, CuS, S(↓)
During I6	Cu_3AsS_4, $Cu_6As_4S_9$, CuS(↓), S
During I7	Cu_3AsS_4

(↓) Very low concentration.
[a] S indicates sulfur glued at the wall of the ampoule.

Temperature dependent powder diffractograms are shown in Fig. 4.

4.2.2. Mechanical treatment

The As_4S_4 + CuS mixture was also subjected to mechanical alloying in a planetary ball mill. Fig. 5 shows some diffractograms and Fig. 6 shows DTA traces of these samples. The diffractograms reveal no products are formed by milling, only the colour of the educts is changing continuously from brown to red over olive-green and dark-gray to black. The broadening half-width of the peaks in the diffractograms indicates a continuous reduction of the particle size.

The DTA trace of the sample prior to milling differs from the trace in Fig. 2 because samples in form of pellets were used. DTA traces of the milled educts reveal strong changes, which indicate that the reaction to Cu_3AsS_4 is shifted to lower temperatures with increasing milling times. After 30 min of milling Cu_3AsS_4 is formed in the DTA within one thermal effect at 330 °C (I3).

4.3. $Cu_{3-x}As$, sulfur, and copper as educts

4.3.1. Thermal synthesis

Typical for educts of group II is a mixture of $Cu_{3-x}As$, sulfur, and copper (reduced at 650 °C). The DTA trace is plotted in Fig. 7, Table 8 contains the products observed in quenched samples. Reaction equations are summarised in Fig. 8.

$Cu_{3-x}As$ reacts already during mortaring with sulfur to Cu_2As and CuS. In freshly prepared mixtures this reaction is completed in the DTA within a small effect at 70 ± 4 °C (II1). The first endothermic effects at 103 ± 1 °C and 117 ± 1 °C (II2 and II3) are due to the α–β transition and melting of sulfur. At 161 ± 2 °C (II4) the main peak reveals the reaction of liquid sulfur and Cu_2As to CuS and arsenic. The reaction of copper powder with sulfur is not detectable due to its little

$$\alpha\text{-}As_4S_4 \xrightarrow{I1} \beta\text{-}As_4S_4$$

$$\beta\text{-}As_4S_4 \xrightarrow{I2} As_4S_4(l)$$

$$3\,As_4S_4(l) + 18\,CuS \xrightarrow{I3,I4} 3\,Cu_6As_4S_9 + 3\,S(g)$$

$$2\,S(g) + 12\,CuS + 2\,Cu_6As_4S_9 \xrightarrow{I5} 8\,Cu_3AsS_4$$

$$6\,CuS \xrightarrow{I6} \frac{6}{2-x}\,Cu_{2-x}S + \frac{6-6x}{2-x}\,S(l)$$

$$\frac{8-7x}{2-x}\,S(l) + \frac{6}{2-x}\,Cu_{2-x}S + Cu_6As_4S_9 \xrightarrow{I7} 4\,Cu_3AsS_4$$

$$36\,CuS + 3\,As_4S_4 \longrightarrow 12\,Cu_3AsS_4$$

Fig. 3. Reactions during heating of the mixture $CuS + As_4S_4$.

extent. The dark-gray grains of the sample are now enveloped by blue-black layers of CuS with residual sulfur on them. The effect II4 is followed by the exothermic reaction of sulfur and intermediate arsenic to As_4S_4 at 275 ± 2 °C (II5). This effect overlaps with melting of As_4S_4, indicated by a step 297 ± 2 °C (II6) in II5. As_4S_4 reacts rapidly with CuS to $Cu_6As_4S_9$ at 306 ± 12 °C (II7). The reproducibility of the onset temperature of II7 and of the following thermal events is not good, revealed by the large standard deviations. After II7 the material is a dark-gray mass. The formation of Cu_3AsS_4 starts at 434 ± 11 °C (II8) from CuS and $Cu_6As_4S_9$. It is probably hindered by protective product layers. At 480 ± 13 °C (II9), besides Cu_3AsS_4 small amounts of Cu_4AsS_5 are formed. The reaction is finished without a detectable thermal effect.

Kuzgibekova et al. [3] synthesised Cu_3AsS_4 from Cu_3As and sulfur. They found exothermic effects at 120, 380, and 520 °C. These results are not comparable with our data, because the authors gave neither heating rates nor the method for the determination of the peak temperatures.

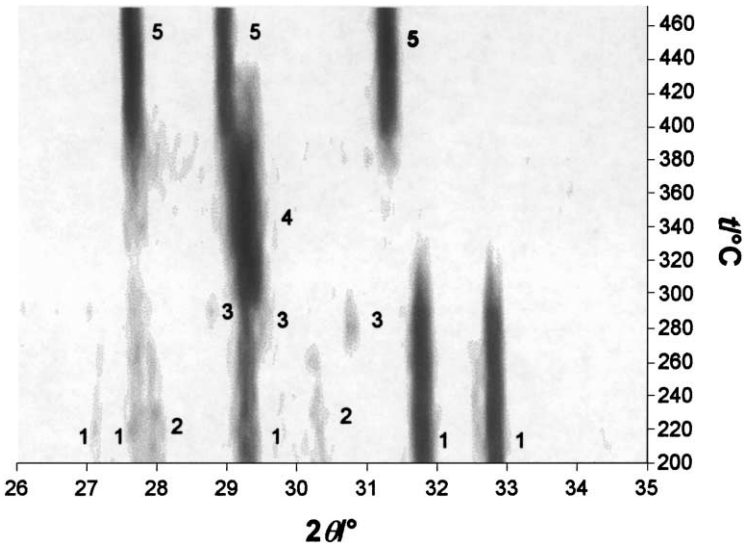

Fig. 4. Temperature dependent diffractograms of the reaction mixture $CuS + As_4S_4$ in Guinier representation. (1) CuS; (2) α-As_4S_4; (3) β-As_4S_4; (4) $Cu_6As_4S_9$; (5) Cu_3AsS_4.

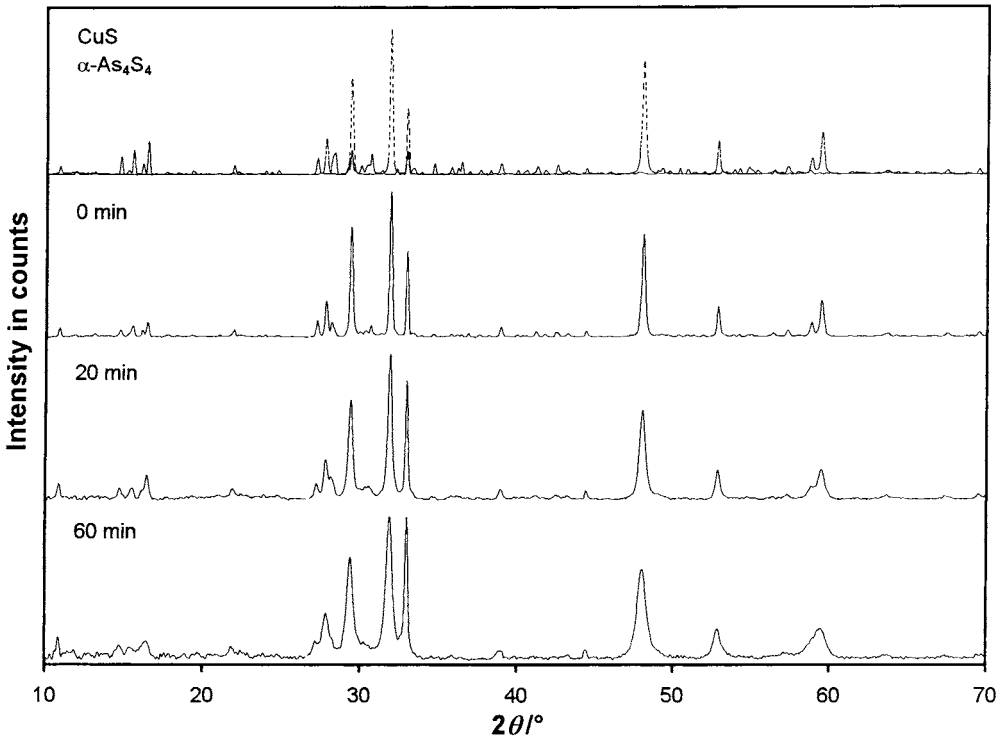

Fig. 5. Diffractograms of the reaction mixture $CuS + As_4S_4$ after different milling times compared with those of the educts.

Fig. 9 depicts a temperature dependent Guinier photograph of the educt mixture. Stability ranges of the compounds obtained from this experiment are given in Table 6. The data confirm the conclusions drawn from the DTA results.

The lower heating rate results in a decrease of reaction temperatures and changes in the product sequence. $Cu_{2-x}S$ is found as further intermediate. The intensities of the X-ray reflections of arsenic decrease without observing new products which contain arsenic. Therefore, amorphous arsenic sulfides must form as intermediates. The final product is $Cu_{12+x}As_{4+y}S_{13}$, instead of Cu_3AsS_4. Its formation may be explained by separation of educts during filling of the quartz capillaries and vaporisation of sulfur.

In addition, diffractograms of the educts were taken at different temperatures. The mixtures were heated with a rate of 5 K/min to a temperature shortly above each reaction effect and equilibrated for 30 min. The observed product sequence was $Cu_6As_4S_9$, $Cu_4As_2S_5$, $Cu_{12+x}As_{4+y}S_{13}$, and Cu_3AsS_4.

4.3.2. Mechanical treatment

Mechanochemical synthesis were investigated with the components $Cu_{3-x}As$ and sulfur. The intrinsic deficiency of copper with regard to the composition Cu_3AsS_4 was not balanced by the addition of copper to simplify the experiments by restriction to two components. The products contained therefore only a mass fraction of 95% Cu_3AsS_4. Using the same pre-treatment DTA traces and temperature dependent X-ray diffractograms of $Cu_{3-x}As + S + Cu$ and $Cu_{3-x}As + S$ are identical within reproducibility. Therefore, the DTA traces in this section were compared with the traces of ground samples shown in Fig. 7.

The reaction mixtures were prepared by mixing carefully with a spatula and afterwards milled in a planetary ball mill. $Cu_{3-x}As$ was used with a particle size in the range 100–36 μm. Fig. 10 depicts diffractograms of milled samples before thermal investigation in comparison with those of educts and final products. Fig. 11 shows the DTA traces of milled samples.

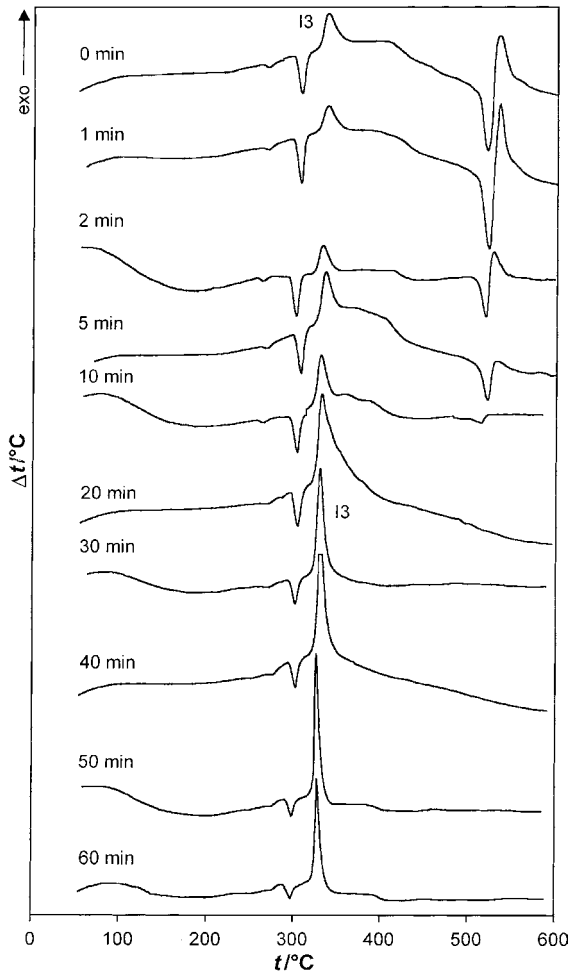

Fig. 6. DTA traces of the reaction mixture $CuS + As_4S_4$ after different milling times.

One diffractogram in Fig. 10 shows a sample which was mixed without mechanical stress (0 min) and instantaneously examined. It reveals that $Cu_{3-x}As$ and sulfur react at the first contact. The most intense reflections are those of $Cu_{3-x}As$(LT) but reflections of $Cu_{5-\delta}As_2$(LT) and Cu_2As are already observed. The reaction is completed during heating to 60 °C (II1). The decaying flank of this effect overlaps with the phase transitions of sulfur. The further reaction path is also influenced by pre-treatment. In the stress free sample, the effects II5 and II7 are separated. An endothermic effect is found at approximately 510 °C, due to the peritectic decomposition of CuS which is followed by an exothermic reaction.

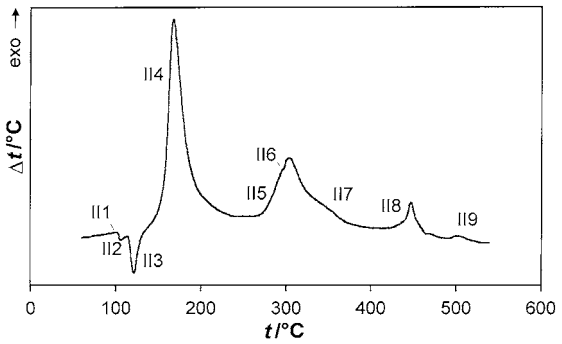

Fig. 7. DTA trace of the reaction mixture $Cu_{3-x}As + S + Cu$.

Similarly to the reaction between $Cu_{3-x}As$ and sulfur during mortaring (Table 4) in the diffractogram of a sample milled for 1 min the reflections of $Cu_{3-x}As$ are substituted by broad reflections of metastable Cu_2As.

The onset temperatures of the effects in the DTA traces change with increasing milling times continuously, though no new products were formed after the first milling period. The small peculiarities within the effect II5 indicate melting of intermediate arsenic sulfides. Only the mean exothermic reaction effect

Table 8
Phases observed in quenched samples of the reaction mixture $Cu_{3-x}As + S + Cu$

Interruption of the reaction	Phases
After grinding, before heating	α-S_8, Cu_2As, Cu(↓), CuS(↓)
Before II2	α-S_8, Cu_2As, CuS(↓), Cu(↓)
After II3	α-S_8, Cu_2As, CuS(↓), Cu(↓)
During II4	As, CuS, α-S_8[a], Cu_2As, S[a], Cu(↓)
After II4	CuS, As, S, α-S_8(↓), Cu(↓), Cu_2As(↓)
Between II4 and II5	CuS, As, S, α-S_8(↓), Cu(↓), β-As_4S_4(↓)
During II6	CuS, As, β-As_4S_4, $Cu_6As_4S_9$, S
During II5	CuS, $Cu_6As_4S_9$, As, β-As_4S_4, S
During II7	CuS, $Cu_6As_4S_9$, As, β-As_4S_4, S(↓)
Between II7 and II8	$Cu_6As_4S_9$, CuS, Cu_3AsS_4(↓), S(↓)
Before II8	$Cu_6As_4S_9$, CuS, Cu_3AsS_4(↓), S(↓)
During II8	Cu_3AsS_4, $Cu_6As_4S_9$, CuS, S(↓)
After II8	Cu_3AsS_4, $Cu_6As_4S_9$, CuS, S(↓)
After II9	Cu_3AsS_4, $Cu_6As_4S_9$, $Cu_4As_2S_5$, CuS(↓), S(↓)
Before melting	Cu_3AsS_4

(↓) Very low concentration.
[a] α-S_8 indicates sulfur indentified by XRD, S indicates sulfur identified with a light microscope.

$$32\ Cu_{3-x}As + (4-4x)\ \alpha\text{-}S_8 \xrightarrow{\text{Grinding, I1}} 32\ Cu_2As + (32-32x)\ CuS$$

$$\alpha\text{-}S_8 \xrightarrow{I2} \beta\text{-}S_8$$

$$\beta\text{-}S_8 \xrightarrow{I3} S_8(l)$$

$$32\ Cu_2As + 8\ S_8(l) \xrightarrow{I4} 64\ CuS + 32\ As$$

$$32x\ Cu + 32x\ S(l) \longrightarrow 32x\ CuS$$

$$32\ As + 32\ S(l) \xrightarrow{I5} 8\ \beta\text{-}As_4S_4$$

$$\beta\text{-}As_4S_4 \xrightarrow{I6} As_4S_4(l)$$

$$48\ CuS + 8\ As_4S_4(l) \xrightarrow{I5, I7} 8\ Cu_6As_4S_9 + 8\ S(l)$$

$$4\ S(g) + 24\ CuS + 4\ Cu_6As_4S_9 \xrightarrow{I8} 16\ Cu_3AsS_4$$

$$2\ S(g) + 16\ CuS + 3\ Cu_6As_4S_9 \xrightarrow{I9} 10\ Cu_3AsS_4 + Cu_4As_2S_5$$

$$2\ S(g) + 8\ CuS + Cu_6As_4S_9 + Cu_4As_2S_5 \longrightarrow 6\ Cu_3AsS_4$$

$$32\ Cu_{3-x}As + 16\ \alpha\text{-}S_8 + 32x\ Cu \longrightarrow 32\ Cu_3AsS_4$$

Fig. 8. Reactions during heating of the mixture $Cu_{3-x}As + S + Cu$.

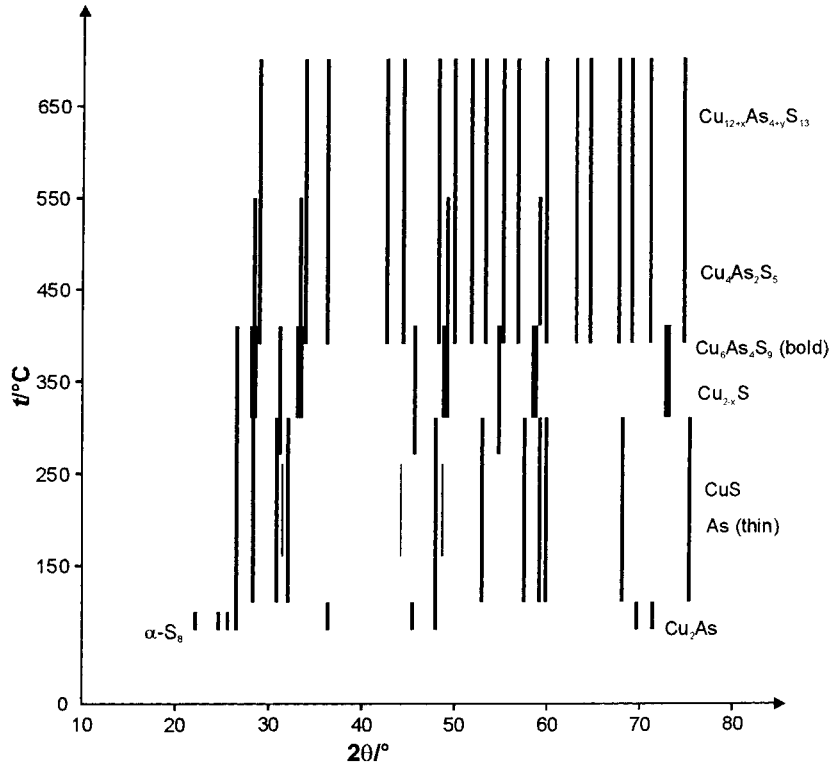

Fig. 9. Schematic representation of a temperature dependent Guinier powder diffractogram of the reaction mixture $Cu_{3-x}As + S + Cu$.

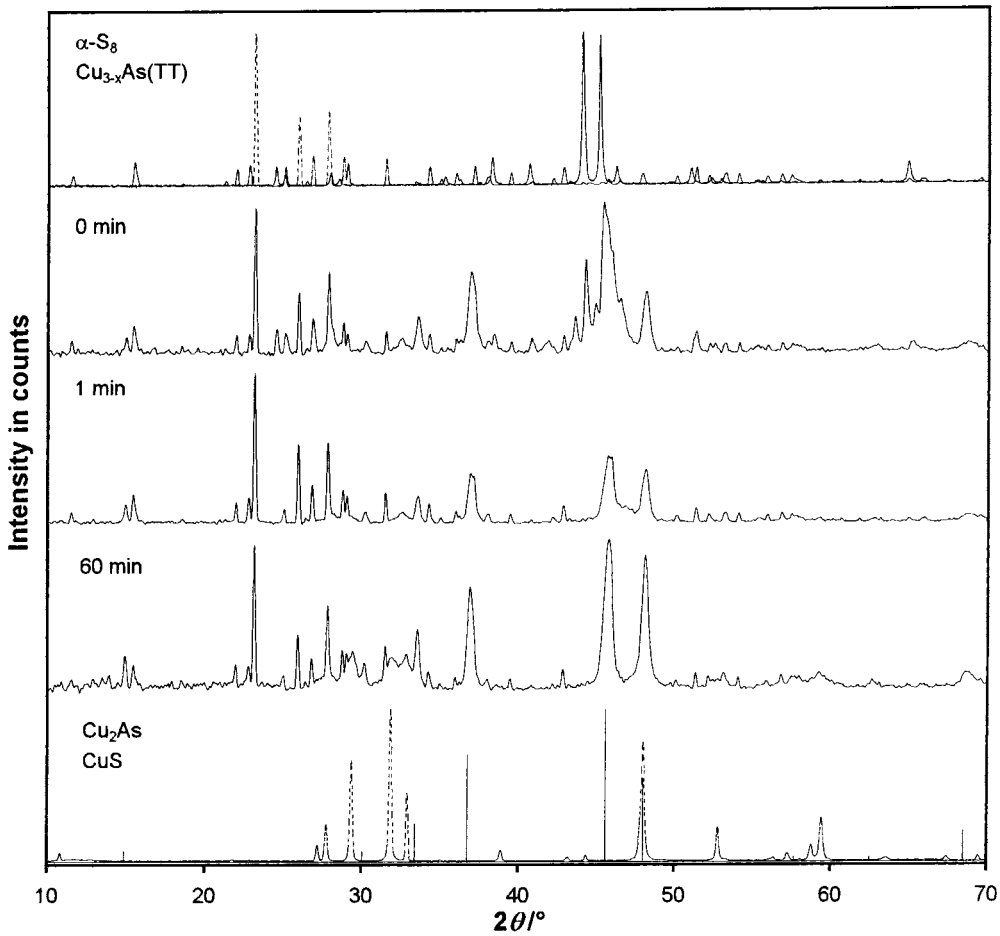

Fig. 10. Diffractograms of the reaction mixtures $Cu_{3-x}As + S$ after different milling times compared with those of educts and products.

(II4) shifts with increasing milling time to higher temperatures, all other exothermic effects drift to lower temperatures with a maximum decrease of about 100 °C.

4.3.3. Other influence factors

Some factors which influence the reaction between $Cu_{3-x}As$ and sulfur to Cu_3AsS_4 were investigated. Similar investigations were performed on the formation of Cu_2S from the elements in previous papers, where details of the procedure are given [23]. The results of both works are compared in Table 9.

The influence of the sample shape on the DTA traces is low for the mixture $Cu_{3-x}As + S$, contrary to the results for the mixture Cu + S. The reproducibility of results is better for $Cu_{3-x}As + S$ pellets, than for powders, opposite to the observation for the Cu + S mixture.

Cu + S react almost completely after a treatment for 60 min in the planetary ball mill, which is not so for $Cu_{3-x}As + S$. In both mixtures the exothermic effects at higher temperatures increase with the size of the particles. The effect is larger for the $Cu_{3-x}As + S$ mixture. The oxygen content of copper plays an important role in synthesis of copper sulfides. It does not influence the reaction to Cu_3AsS_4, because traces of oxygen are removed during the preparation of $Cu_{3-x}As$.

Whether factors like atmosphere or irridation are important as for Cu + S mixtures remains unclear,

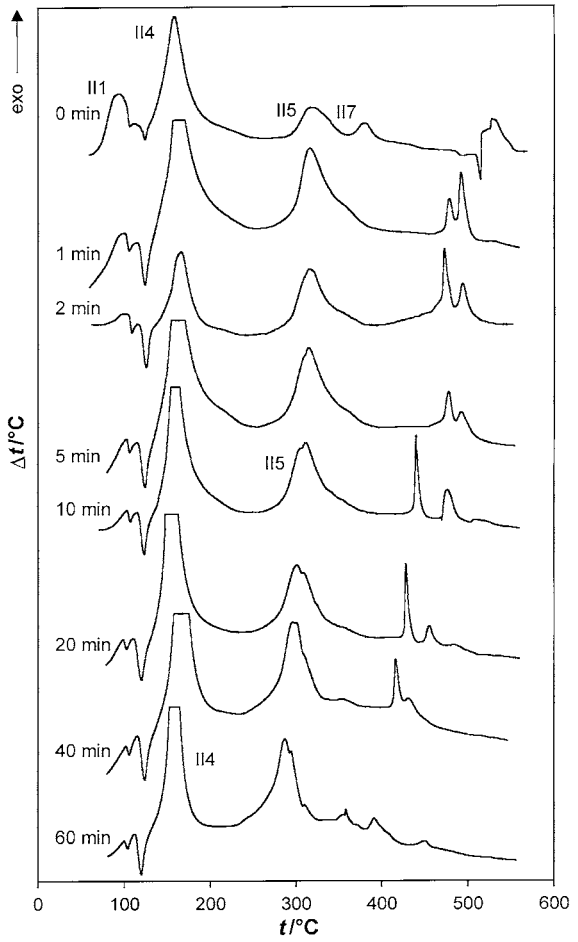

Fig. 11. DTA traces of the reaction mixture $Cu_{3-x}As + S$ after different milling times.

because of the rapid reaction between $Cu_{3-x}As$ and sulfur. Onset temperatures and intensities of reaction peaks shift to higher temperatures with increasing heating rate for the copper arsenide mixtures. In the synthesis of Cu_2S only the onset temperatures increase, reaction peak intensities drift to lower temperatures.

4.4. Elements as educts

4.4.1. Thermal synthesis

Finally, the reaction of the constituent elements (copper powder reduced at 650 °C) to Cu_3AsS_4 is described. The DTA trace is given in Fig. 12 and the reaction products found after quenching in Table 10. Sulfur rich $Cu_{2-x}S$ transformed during quenching into $Cu_{1.8}S$ and copper rich $Cu_{2-x}S$ into $Cu_{1.95}S$, $Cu_{1.96}S$, or α-Cu_2S. Reaction equations are summarised in Fig. 13. The formula Cu_2S is used instead of $Cu_{2-x}S$ for simplification.

The mixture turns gray on mortaring due to the formation of CuS. This reaction can also cause a small exothermic effect at 81 ± 4 °C (III1) in freshly prepared mixtures. Next thermal events are the α–β transition at 103 ± 1 °C (III2) and melting (III3) of sulfur at 119 ± 2 °C. The reaction proceeds with the formation of small amounts of CuS at 165 ± 3 °C (III4). The main thermal effect (III5) at 195 ± 2 °C includes three different reactions. First of all more CuS is formed which can be recognised by deep blue colouring of the mixture. CuS reacts simultaneously in two ways, with arsenic and sulfur to $Cu_6As_4S_9$ and with unconsumed copper to $Cu_{2-x}S$. Though enough sulfur is present to consume all copper to form CuS, after III5 larger amounts of $Cu_{2-x}S$ than of CuS are observed in the diffractograms. The sample consists now of blue-black globules, which are surrounded by gray globules and sulfur. At 260 ± 4 °C (III6) residual arsenic reacts with sulfur to arsenic sulfides mainly As_4S_4 in form of orange crystals. Prior to melting As_4S_4 seems to react with CuS to sinnerite, $Cu_6As_4S_9$ (III6). This reaction cannot be definitely deduced from the experimental observations, but it is probable because it is found in the mixtures $CuS + As_4S_4$ and $Cu_{3-x}As + S + Cu$ at this temperature. $Cu_6As_4S_9$ and $Cu_{2-x}S$ are main components of the mixture when residual As_4S_4 melts at 304 ± 1 °C (III7). During the slow decay of the effect III6, the decay is marked by III8 in Fig. 12, As_4S_4 reacts with sulfur to amorphous As_2S_3 which can be recognised by the glassy dark-red or black regions instead of the orange ones in the quenched sample. Though between III6 and III9 no thermal effects are found in the DTA traces. Quenching experiments revealed that the reaction is proceeding; at first $Cu_{2-x}S$ and arsenic sulfides and then $Cu_{2-x}S$ and $Cu_6As_4S_9$ react to Cu_3AsS_4 and with a lesser extent to $Cu_4As_2S_5$. The CuS content remains constant. These reactions can occur without detectable thermal effect because the enthalpies of formation of the educts $Cu_{2-x}S$ and $Cu_6As_4S_9$ are very high, so that the reaction enthalpies are probably very low. The peritectic decomposition of CuS at 505 ± 5 °C (III))

Table 9
Comparison of influence parameters on the reaction mixtures $Cu_{3-x}As + S$ and $2Cu + S$ [23]

Influence parameter	$Cu_{3-x}As + S \rightarrow$ '$Cu_{2.81}AsS_{3.81}$'	$2Cu + S \rightarrow Cu_2S$
Form of sample[a] (powder or pellet)	Differences only in regions with generally less reproducibility	Very important for shape and onset temperatures
Reproducibility (°C)[b]	Powders: ±6.3, pellets: ±1.4	Powders: ±3.5, pellets[c]: ±3.4
Mechanical treatment	Accelaration only during beginning of reaction even by grinding	Complete conversion possible by milling
Particle size	Very important	Very important
Purification	$Cu_{3-x}As$	Copper: very important at least for copper oxides
	Sulfur: very small influence	Sulfur: very small influence
Sources of educts (after purification)	$Cu_{3-x}As$[d]: no influence	Copper: important because of very different particle shapes
	Sulfur: no influence	Sulfur: no influence
Ageing	Accelaration only in the beginning of the reaction	Complete conversion possible within weeks. Atmosphere (argon, vaccuum) and light irradiation also very important
Heating rate	Very important	Very important
Self-propagating reaction	No complete conversion possible	Complete conversion possible by using fine particles

[a] According to DTA-curves.
[b] Standard deviations of onset temperature DTA-curves, ±0.8 °C for phase transitions. Valid for samples from the same educt mixture [23].
[c] Above all reproducibility of peak shape is small.
[d] Different synthesis condition particular temperatures.

induces the final reaction to Cu_3AsS_4 (III10) at 524 ± 1 °C.

Temperature dependent Guinier photographs were obtained up to a temperature of ca. 370 °C, above that the quartz capillaries with the elementary educts fragmented. The reaction sequence changed with the low heating rate. Above 200 °C CuS was consumed in favour of $Cu_{2-x}S$ and $Cu_{12+x}As_{4+y}S_{13}$. The latter was observed only in this case as primary ternary intermediate in DTA runs.

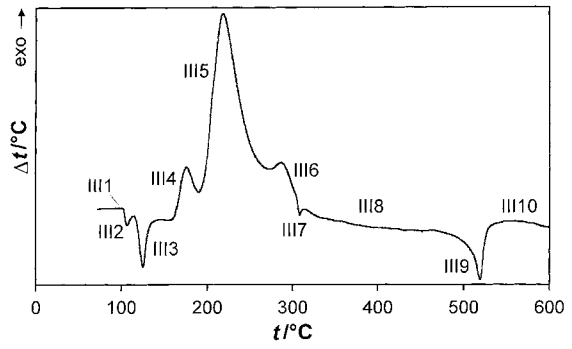

Fig. 12. DTA trace of the reaction mixture Cu + S + As.

4.4.2. Influence of desoxidation of copper

The reaction mixture Cu + As + S was also investigated using copper powder as received, reduced at 260 and 650 °C. Copper which was reduced at 260 °C still contains eutectic Cu_2O [23]. The DTA traces are shown in Fig. 14. The first exothermic reaction (III4) occurs only with oxygen-free copper powders. A comparison of mixtures with copper powders treated at 260 and 650 °C shows a shift of the intensity of reaction peaks to higher temperatures, whereas the onset temperatures of thermal effects are nearly identical up to the melting of As_4S_4 (III7).

Due to the oxygen film on untreated copper, the main exothermic reaction below 350 °C is that of arsenic with sulfur to arsenic sulfides (III6). The reaction of the sulfides and residual sulfur with copper to Cu_3AsS_4 occurs at much higher temperature (411 °C) than in the previously reduced copper powders.

In reaction mixtures with untreated copper as well as with those with copper powders reduced at 260 °C the decomposition of CuS is not observed.

Table 10
Phases observed in quenched samples of the reaction mixture Cu + S + As

Interruption of the reaction	Phases
After grinding, before heating	Cu, As, α-S_8, CuS(↓)
Before III2	Cu, As, α-S_8, CuS(↓)
After III3	Cu, As, α-S_8, CuS(↓)
Before III4	Cu, As, α-S_8, CuS(↓)
During III4	Cu, As, α-S_8 CuS(↓)
After III4	Cu, As, CuS, S[a], α-S_8(↓)
During III5	As, Cu, CuS, S, $Cu_6As_4S_9$(↓)
After III5	As, $Cu_6As_4S_9$, $Cu_{1.8}S$, CuS, S, Cu(↓)
During III6	$Cu_6As_4S_9$, As, $Cu_{1.8}S$, CuS, β-As_4S_4, Cu(↓), S(↓)
During III7	$Cu_6As_4S_9$, $Cu_{1.8}S$, As, CuS, As_4S_4[b], β-As_4S_4(↓), S(↓)
After III7	$Cu_6As_4S_9$, $Cu_{1.8}S$, As, CuS, As_4S_4, β-As_4S_4(↓), S(↓)
During III8	$Cu_6As_4S_9$, CuS, $Cu_{1.8}S$, As_2S_3, As_4S_4, As(↓), β-As_4S_4(↓), Cu_3AsS_4(↓)
Before III9	Cu_3AsS_4, $Cu_4As_2S_5$, CuS, As_2S_3, $Cu_{1.8}S$(↓)
After III9	Cu_3AsS_4, $Cu_4As_2S_5$, S, As_2S_3, $Cu_{1.8}S$(↓)
During III10	Cu_3AsS_4, Cu_4AsS_5, $Cu_{1.8}S$, As_2S_3, S(↓)
Before melting	Cu_3AsS_4, S(↓)

(↓) Very low concentration.
[a] α-S_8 indicates sulfur indentified by XRD, S indicates sulfur identified with a light microscope.
[b] β-As_4S_4 indicates arsenic tetrasulfide indentified by XRD, As_4S_4 indicates arsenic tetrasulfide identified with a light microscope.

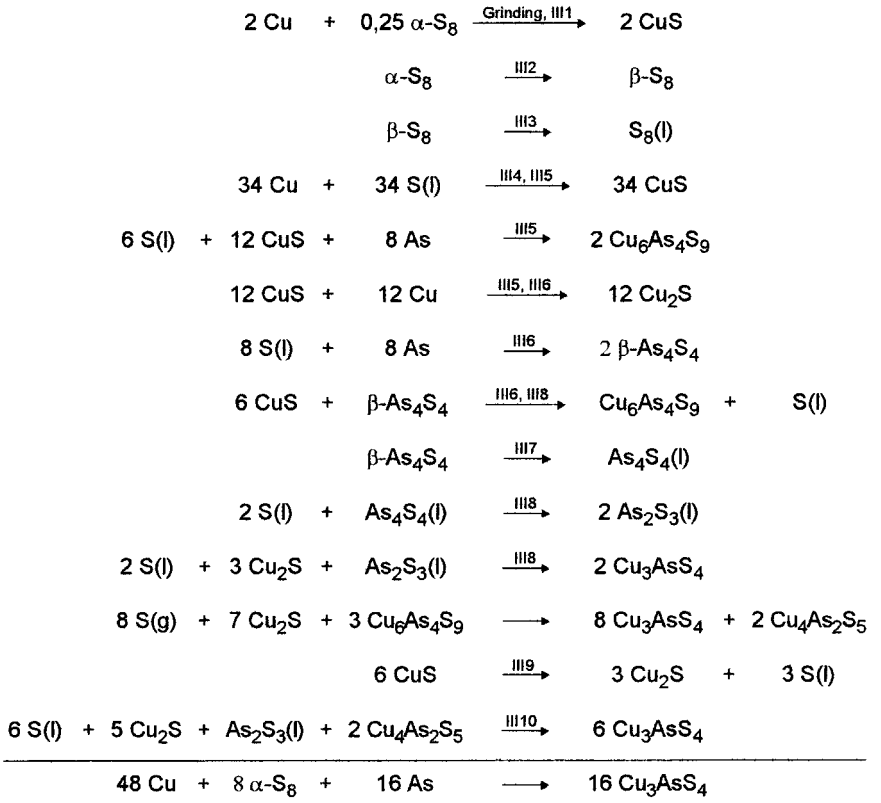

Fig. 13. Reactions during heating of the mixture Cu + S + As.

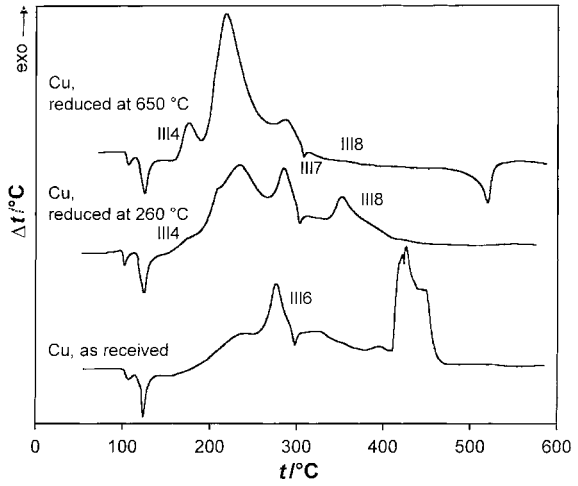

Fig. 14. DTA traces of reaction mixtures Cu + S + As with copper powders of different oxygen content.

Acknowledgements

The authors appreciate financial support by the Deutsche Forschungsgemeinschaft and thank Tatiana Mikhailopoulo for translating the Russian literature.

References

[1] S.M. Isabaev, A.N. Polukarov, K. Kuzgibekova, Deposited Document, VINITI 5161-80, 1981.
[2] A.G. Fitzgerald, Thin Solid Films 98 (1982) 101.
[3] K. Kuzgibekova, L.F. Sivak, S.M. Isabaev, Kompleksn, Ispol'z Miner, Syrya, Vol. 48, 1993.
[4] R.T. Shuey, Semiconducting ore minerals, Elsevier, New York, USA, 1975, p. 331.
[5] J. Falbe, M. Regitz, C.D. Römpp Chemie-Lexikon, Version 1.0, Thieme, Stuttgart, 1995.
[6] H. Kleinheisterkamp, Z. Erzbergbau Metallhüttenwesen 1 (1948) 65.
[7] J. Gerlach, U. Henning, K. Trettin, Z. Erzbergbau Metallhüttenwesen 19 (1966) 458.
[8] L. Cambi, M. Elli, Chim. Ind. (Milan) 49 (1967) 606.
[9] S. Maske, B.J. Skinner, Econ. Geol. 66 (1971) 901.
[10] N.I. Kopylov, S.M. Minkevich, M.Z. Toguzov, D.B. Smailov, Russian J. Inorg. Chem. 20 (1975) 1878.
[11] B. Gather, R. Blachnik, J. Less-Common Met. 48 (1976) 205.
[12] G. Kurz, Ph.D. Thesis, Universität Siegen, 1984.
[13] G. Kurz, R. Blachnik, J. Less-Common Met. 155 (1989) 1.
[14] M. Rikel', M. Harmelin, A. Prince, in: G. Petzow, G. Effenberg, F. Aldinger (Eds.), Ternary Alloys, Vol. 10, VCH, Weinheim, 1994, p. 109.
[15] G. Adiwidjaja, J. Löhn, Acta Crystallogr. B26 (1970) 1878.
[16] A. Edenharter, Schweiz. Mineral Petrog. Mitt. 56 (1976) 195.
[17] F.D. Luce, C.L. Tuttle, B.J. Skinner, Econ. Geol. 22 (1977) 271.
[18] R.A.D. Pattrick, G. van der Laan, D.J. Vaughan, C.M.B. Henderson, Phys. Chem. Minerals 20 (1993) 395.
[19] B. Gather, Ph.D. Thesis, Techn. Universität Clausthal, 1976.
[20] PDF-2 Database, International Centre for Diffraction Data, PA, USA, 1996.
[21] Inorganic Crystal Structure Database, Release 98/2, FIZ Karlsruhe, Gmelin Institute, 1998.
[22] Stoe and Cie GmbH, Version 3.01, Darmstadt, 1996.
[23] R. Blachnik, A. Müller, Thermochim. Acta 361 (2000) 31.
[24] J.E. Dutrizac, R.J.C. MacDonald, Mater. Res. Bull. 8 (1973) 961.
[25] K. von Benda, R. Juza, Z. Anorg. Allg. Chem. 371 (1969) 172.
[26] Inorganic Crystal Structure Database, Release 98/2, File 26776, FIZ Karlsruhe, Gmelin Institute, 1998.
[27] P.R. Subramanian, D.E. Laughlin, Bull. Alloy Phase Diag. 9 (1988) 605.
[28] R. Juza, K. von Benda, Z. Anorg. Allg. Chem. 357 (1968) 238.
[29] R. Blachnik, A. Hoppe, U. Wickel, Z. Anorg. Allg. Chem. 463 (1980) 78.
[30] B. Voigt, B. Jacob, Monatshefte Chem. 113 (1982) 895.
[31] T.B. Massalski, in: T.B. Massalski (Ed.), Binary Alloys Phase Diagrams, 2nd Edition, Vol. 1, ASM International, USA, 1992, p. 314.
[32] J. Wypartowicz, K. Fitzner, O.J. Kieppa, J. Alloys Compd. 217 (1995) 1.
[33] I. Barin, Thermochemical Data of Pure Substances, Vol. 2, VCH, Weinheim, 1989, p. 489.
[34] J.H. Wernick, K.E. Benson, J. Phys. Chem. Solids 3 (1957) 157.
[35] L.G. Berg, E.N. Shlyapkina, J. Therm. Anal. 8 (1975) 417.
[36] K.Z. Zhumashev, Inorg. Mater. 28 (1992) 325.
[37] PDF-2 Database, File 05-632, International Centre for Diffraction Data, PA, USA, 1996.
[38] P.R. Subramanian, D.E. Laughlin, in: T.B. Massalski (Ed.), Binary Alloys Phase Diagrams, 2nd Edition, Vol. 1, ASM International, USA, 1992, p. 271.
[39] PDF-2 Database, File 21-0280, International Centre for Diffraction Data, PA, USA, 1996.
[40] W. Liebisch, K. Schubert, J. Less-Common Met. 23 (1971) 231.
[41] PDF-2 Database, File 41-1494, International Centre for Diffraction Data, PA, USA, 1996.
[42] Inorganic Crystal Structure Database, Release 98/2, File 15238, FIZ Karlsruhe, Gmelin Institute, 1998.
[43] PDF-2 Database, File 24-0078, International Centre for Diffraction Data, PA, USA, 1996.
[44] Inorganic Crystal Structure Database, Release 98/2, File 16092, FIZ Karlsruhe, Gmelin Institute, 1998.
[45] PDF-2 Database, File 42-0537, International Centre for Diffraction Data, PA, USA, 1996.
[46] D.J. Chakrabarti, D.E. Laughlin, in: T.B. Massalski (Ed.), Binary Alloys Phase Diagrams, 2nd Edition, Vol. 2, ASM International, USA, 1992, p. 1467.

[47] PDF-2 Database, File 06-0464, International Centre for Diffraction Data, PA, USA, 1996.
[48] Inorganic Crystal Structure Database, Release 98/2, File 100333, FIZ Karlsruhe, Gmelin Institute, 1998.
[49] PDF-2 Database, File 29-0578, International Centre for Diffraction Data, PA, USA, 1996.
[50] PDF-2 Database, File 41-0959, International Centre for Diffraction Data, PA, USA, 1996.
[51] Inorganic Crystal Structure Database, Release 98/2, File 100334, FIZ Karlsruhe, Gmelin Institute, 1998.
[52] PDF-2 Database, File 08-0247, International Centre for Diffraction Data, PA, USA, 1996.
[53] PDF-2 Database, File 25-0266, International Centre for Diffraction Data, PA, USA, 1996.
[54] PDF-2 Database, File 36-1490, International Centre for Diffraction Data, PA, USA, 1996.
[55] PDF-2 Database, File 35-0775, International Centre for Diffraction Data, PA, USA, 1996.
[56] B.J. Wünsch, Y. Takeuchi, W. Nowacki, Z. Kristallogr. 123 (1966) 1.
[57] PDF-2 Database, File 24-0061, International Centre for Diffraction Data, PA, USA, 1996.
[58] Inorganic Crystal Structure Database, Release 98/2, File 202785, FIZ Karlsruhe, Gmelin Institute, 1998.